Heriot-Watt University

Heriot-Watt University
Research Gateway

Miniature Quasi-Lumped-Element Wideband Bandpass Filter at 0.5–2-GHz Band Using Multilayer Liquid Crystal Polymer Technology

Hong, Jia-Sheng; Qian, Shilong

Published in:
IEEE Transactions on Microwave Theory and Techniques

DOI:
10.1109/TMTT.2012.2205939

Publication date:
2012

Link to publication in Heriot-Watt Research Gateway

Citation for published version (APA):
Hong, J-S., & Qian, S. (2012). Miniature Quasi-Lumped-Element Wideband Bandpass Filter at 0.5–2-GHz Band Using Multilayer Liquid Crystal Polymer Technology. IEEE Transactions on Microwave Theory and Techniques, 60(9), 2799-2807. 10.1109/TMTT.2012.2205939

Miniature Quasi-Lumped-Element Wideband Bandpass Filter at 0.5–2-GHz Band Using Multilayer Liquid Crystal Polymer Technology

Shilong Qian, *Student Member, IEEE*, and Jiasheng Hong, *Fellow, IEEE*

***Abstract*—Miniature wideband bandpass filters are proposed using multilayer liquid crystal polymer (LCP) technology to cover the very low-frequency band of 0.5–2 GHz. To reduce the filter size at such low frequencies, lumped-element theory is used for the filter design and a value extraction process is developed to accurately get the capacitive or inductive values of different multilayer microstrip quasi-lumped elements. These elements are used to produce the required filter response, and thus the overall design process relies less on the time-consuming EM optimization. A filter with the size $0.058\ \lambda_g \times 0.026\ \lambda_g \times 0.004\ \lambda_g$ is demonstrated as an initial design. To further improve the stopband performance, an improved design is then developed while still maintaining the compact sizes within $0.065\ \lambda_g \times 0.026\ \lambda_g \times 0.004\ \lambda_g$. Both filters are fabricated on a five-metal layer LCP construction, which has not been done before, with robust via connections using the newly developed laser-aided fabrication technique. Good agreements between simulation and fabrication are observed, which has proven both the success of the design methodology, as well as the fabrication technique.**

***Index Terms*—Bandpass filter, liquid crystal polymer (LCP), miniature filter, ultra-wideband (UWB) filter.**

I. Introduction

BANDPASS filters are essential and critical parts of communication and radar systems. Apart from the usual requirements for low loss and high selectivity, for a highly integrated system, it is more desirable that the filters are very small and compatible with the normal printed circuit board (PCB) processing, so they can be easily integrated into a system.

Recently, there is an increasing demand for such miniature and high-performance wideband filters to operate at low frequencies band, e.g., 0.5–2 GHz, for some emerging applications, such as wideband radar. However, considering the large wavelengths at these frequencies, conventional planar filters usually occupy large circuit board area and are high cost.

During the past ten years, with the development of novel multilayer packaging material, multilayer compact bandpass filters have been developed in [1]–[13]. As a very mature and popular technology, low-temperature co-fired ceramic (LTCC) has been attracting many people's interest in microwave circuit design. LTCC has high dielectric constant (up to 10.2) and low dielectric loss (between 0.002–0.004), which provide a very promising solution for compact passive filter design within a small format [1]–[3]. In these publications, filters are designed in a novel 3-D format on multilayer LTCC substrates, thus the sizes of filters are reduced dramatically. However, these ultra compact filters are for narrowband applications. In [4] and [5], wideband filters have been investigated using LTCC. However, the fractional bandwidth (FBW) of 45% in [4] is still not wide enough, while [5] requires extremely high fabrication accuracy due to the use of 70-μm quarter-wavelength coupled lines, which would be too narrow for multilayer laminated circuit fabrication.

Besides LTCC, an organic substrate is an option for small size filter design, such as the very recent RXP organic substrate [6], [7]. RXP substrate has a low dielectric constant between 3–3.5 at around 1 GHz and very low processing temperature around 220 °C, which is very suitable for RF modules integration [6]. However, as a new technology, the filter design in [7] was not able to produce a sharp passband edge. Furthermore, the stopband is quite narrow and the rejection is not good enough.

Another organic candidate, liquid crystal polymer (LCP), has also been popular due to its superior electrical properties up to millimeter-wave frequencies [8]–[14]. It has a stable low dielectric constant around 3 and low dielectric loss tangent 0.0025 over a wide frequency range. These properties make LCP a very suitable solution for compact wideband filter designs [10]–[13]. Compared to LTCC, LCP has much lower processing temperature around 280 °C. Although LCP has lower dielectric constant than LTCC, which makes it more challenging for RF/microwave circuit miniaturization, it makes LCP circuit design less sensitive to fabrication tolerances than LTCC, which is very important for multilayer laminated circuit. Although some cheaper PCB laminates can be used for miniature filter designs, as in [15], LCP offers much higher flexibility on circuit thickness and a very strong coupling can be achieved with a separation as small as 25 μm. This is very important for the design of low-frequency wideband filters that requires large capacitances. Furthermore, in the LCP adhesive system, circuit layers (core films) and prepreg layers (bonding films) have almost the same characteristics, such as thermal expansion coefficient, dielectric constant, and water absorption, which can be a great benefit for both filter designs and practical applications. Table I lists some typical miniature filters in terms of the technology, size, and performances.

Although ultra-wideband (UWB) LCP filters operating at frequencies between 3.1–10.6 GHz have been reported in

Manuscript received April 20, 2012; revised May 31, 2012; accepted June 06, 2012. Date of publication July 11, 2012; date of current version August 28, 2012.

The authors are with the Department of Electrical, Electronic and Computer Engineering, Heriot-Watt University, Edinburgh EH14 4AS, U.K. (e-mail: sq31@hw.ac.uk).

Color versions of one or more of the figures in this paper are available online at http://ieeexplore.ieee.org.

Digital Object Identifier 10.1109/TMTT.2012.2205939

0018-9480/$31.00 © 2012 IEEE

TABLE I
COMPARISON OF VARIOUS MINIATURE WIDEBAND BANDPASS FILTERS

Reported Miniature Bandpass Filter in reference		Fabrication Technology	Passband Bandwidth (GHz) and FBW	Circuit Size (λ_g^3) at Center Frequency	Number of Metallization Layers	Insertion Loss	10 dB Upper Stopband FBW
[4]		Multilayer LTCC	3.1-4.9 45%	0.203 × 0.079 × 0.031	11	< 1.1 dB	Wider than 177.5%
[5]		Multilayer LTCC	3.1-10.6 110%	0.574 × 0.574 × 0.020	5 (2 Grounds)	< 0.8 dB	Wider than 110%
[7]		Multilayer RXP	4.85 – 6.35 27%	0.055 × 0.047 × 0.006	4	0.92 dB at 5.6 GHz	Narrower than 48%
[11]		Multilayer LCP	3.1-10.6 110%	0.359 × 0.207 × 0.014	3	0.35 dB at 6.85 GHz	146%
[15]		Multilayer PCB	7.5-12.5 50%	0.583 × 0.578 × 0.1	5 (2 Grounds)	About 1 dB	Wider than 25%
This Work	1st Design	Multilayer LCP	0.5 - 2 120%	0.058 × 0.026 × 0.004	5	< 0.7 dB	360%
	2nd Design			0.065 × 0.026 × 0.004		< 0.7 dB	400% (2 transmission zeros)

[10]–[13], to the authors' knowledge, miniature wideband bandpass LCP filters for low RF/microwave frequencies have not been investigated and the large wavelengths at these frequencies make it very challenging for size reduction while maintaining a good performance. For an UWB filter, compact design with a size smaller than 10 mm × 5 mm has been reported in [11], thus this work is aimed to develop a wideband bandpass filter covering a much lower frequency band from 0.5 to 2 GHz while still keeping the same size as in [11] to achieve about 80% size reduction.

To achieve this, implementing the filter on more layers is a feasible solution. However, in the open literature, most LCP microwave filters have only been implemented with two circuit layers and a ground plane [10]–[14], and very little has been reported for the LCP microwave filter with more than two circuit layers [16]. An obvious reason for this is due to the less mature LCP fabrication process when more circuit layers are used. Thus, developing a reliable fabrication process for LCP multilayer circuits is another objective of this work, and a design implemented with four circuit layers and a ground plane will be discussed in this paper with the complete fabrication process.

The detailed design methodology and multilayer elements analysis are presented in Section II; based on these elements, a high-pass (HP) filter with 0.5-GHz cutoff and a low-pass (LP) filter with 2-GHz cutoff are presented and then cascaded in Section III to achieve the required bandpass response. For the multilayer structure, a newly developed fabrication technique is discussed in Section IV. Measured results are discussed in Section V and are followed by a conclusion in Section VI.

II. QUASI-LUMPED-ELEMENT DESIGN

For compact filter design at low frequencies, distributed element resonators are not suitable due to their large sizes, which are comparable to the wavelengths, thus microstrip quasi-lumped-elements are usually used to design small size filters.

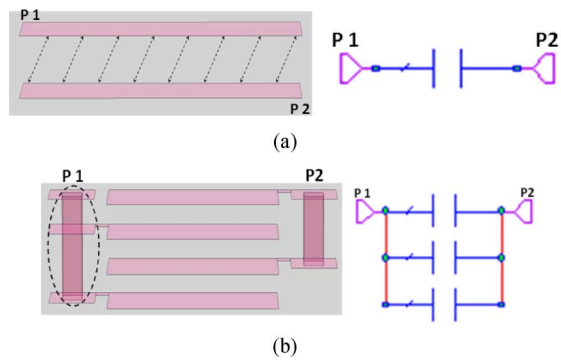

Fig. 1. (a) Conventional broadside coupling structure. (b) Multilayer broadside coupling structure on multilayer LCP.

A. Quasi-Lumped-Elements on Multilayer LCP Substrate

The capacitors are usually the most size consuming parts in a conventional single-layer filter design, where only weak edge coupling such as that in an interdigital capacitor is adopted. This becomes a more serious problem for a low-frequency filter design, where large capacitances are needed. With the development of multilayer substrate, strong broadside coupling structures can be easily implemented, which reduces the size of the capacitive elements dramatically. As shown in Fig. 1(b), the four-layer structure [18], [19] works as three capacitors paralleled between two ports, which theoretically can reduce the size by 67% compared to the structure in Fig. 1(a). Further size reduction can be achieved by using more layers with the cost of fabrication complexity.

Fig. 2 shows the microstrip inductors that are used in this work. The meander line can be used to implement small series inductance between any two ports while the spiral line [20], with a connection via, are very suitable for realizing large shunt inductance between any two layers in a multilayer circuit design or to the ground.

B. Element Value Extraction

Before building these elements together for the proposed filter, it would be ideal if these elements have accurate values

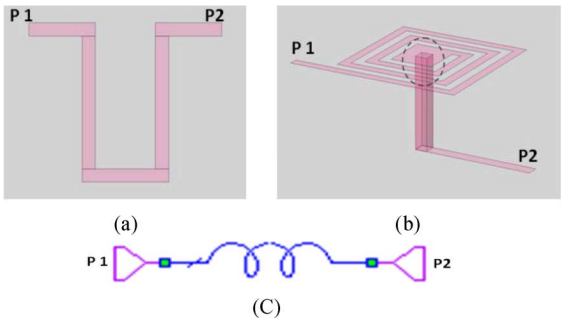

Fig. 2. Microstrip inductors. (a) Meander and (b) rectangular spiral high-impedance lines. (c) Circuit model.

as required by the circuit prototype so that even the initially designed filter can produce similar response as the circuit prototype, and the design cycle can rely less on the time consuming electromagnetic (EM) optimization. Although many closed-form formulas are available in [17] and [18] to calculate element values, in a practical design, some small parts of these elements, such as the vias and via patches, shown as dashed circles in Figs. 1(b) and 2(b), may be customized for the consideration of easy fabrication and clear layout, thus it would be difficult for formulas to include the effect of these parts. To solve this and get more accurate control of the element values during the design cycle, a microstrip element value extraction process, first shortly introduced in [16], is used in this work to obtain a connection between the microstrip elements and their capacitances or inductances.

It should be mentioned that there will always be coupling between these elements and the ground, but due to the low dielectric constant of the substrate, by using a relatively large separation, these coupling capacitances are much smaller than the main series inductances/capacitances.

III. Bandpass Filter Design

To start the wideband bandpass filter design with bandwidth from 0.5 to 2 GHz, which gives an FBW 120% at center frequency of 1.25 GHz, a lumped-element filter prototype, which consists of an HP and LP section, has been chosen to produce the required response, as shown in Fig. 3(a).

Since the cutoff frequencies of these two sections are chosen separately, the design method of this work can be readily applied to other frequency design. In addition, with a properly designed LP section, a wide upper stopband can be easily achieved. Compared to the resonators-based bandpass filter, this cascaded type of bandpass filter can provide small and flat group delay [11]. Regarding the choices of the HP and LP sections, the consideration will be discussed in the following sections. The listed HP and LP elements values are optimized with the initial values obtained from LP prototypes, respectively, through frequency and elements transformation. The filter will be implemented on multilayer LCP substrate with a total thickness of 0.6 mm, and the relative dielectric constant and loss tangent for the LCP are 3 and 0.0025, respectively.

A. HP Section Design

Since size reduction has been the main challenge of this work, the first consideration on choosing an appropriate prototype is

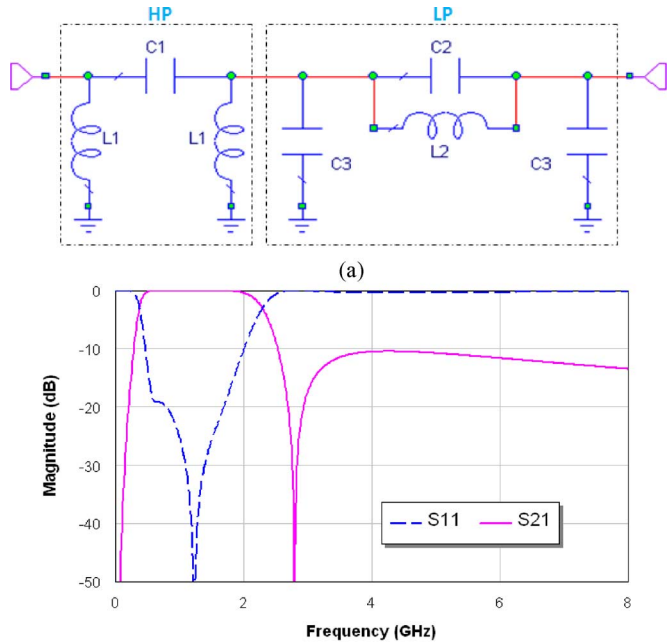

Fig. 3. (a) Proposed circuit prototype and (b) its simulation response ($C1 = 5.5$ pF, $L1 = 14.3$ nH, $C2 = 1.33$ pF, $L2 = 2.48$ nH, $C3 = 1.19$ pF).

the total number of elements in the prototype. Potentially, the less number of elements, the smaller the footprint of the filter implementation, though there may be some tradeoff for the selectivity and out-of-band rejection.

Based on this, for the HP section, the π network, as shown in Fig. 3(a), is chosen to produce a Chebyshev HP response with 0.5-GHz cutoff. For the Chebyshev HP filter, since there is always a transmission zero located at dc, this simple HP prototype can produce a sharp passband edge for the 0.5-GHz cutoff, as shown in Fig. 3(b).

For the relatively large capacitance $C1$ in Fig. 3(a), a four-layer broadside-coupled capacitor, as shown in Fig. 1(b) with planar dimensions in Fig. 4(a), is chosen. The separation d between every two layers is chosen to be 0.05 mm for a strong coupling, while the substrate has a relative dielectric constant $\varepsilon_r = 3$ and total thickness $h = 0.6$ mm (i.e., from the top circuit layer to the ground). The sizes of the via and via patches are mainly for the consideration of easy fabrication. The initial values of W and L are chosen according to the metal–insulator–metal (MIM) capacitance formula of (1), where n is the number of layers. Since this only gives a rough design, then by varying W and L, more accurate capacitor values can be extracted using the method as mentioned in Section II-B, and the $L = 2.6$ mm and $W = 1.1$ mm combination can be chosen to realize $C1$ in the circuit prototype. Fig. 4(b) shows the capacitances and Q factors of the selected combination, extracted from simulation, at different frequencies near the cutoff frequency 0.5 GHz, for the substrate loss tangent $\tan\delta = 0.0025$ and the conductor conductivity $\sigma = 5.8 \times 10^7$ S/m

$$C = \frac{\varepsilon \times [W \times L \times (n-1)]}{d}. \tag{1}$$

For the large inductance $L1$, a high-impedance spiral line should be used for a compact design. Since the inductor $L1$ is

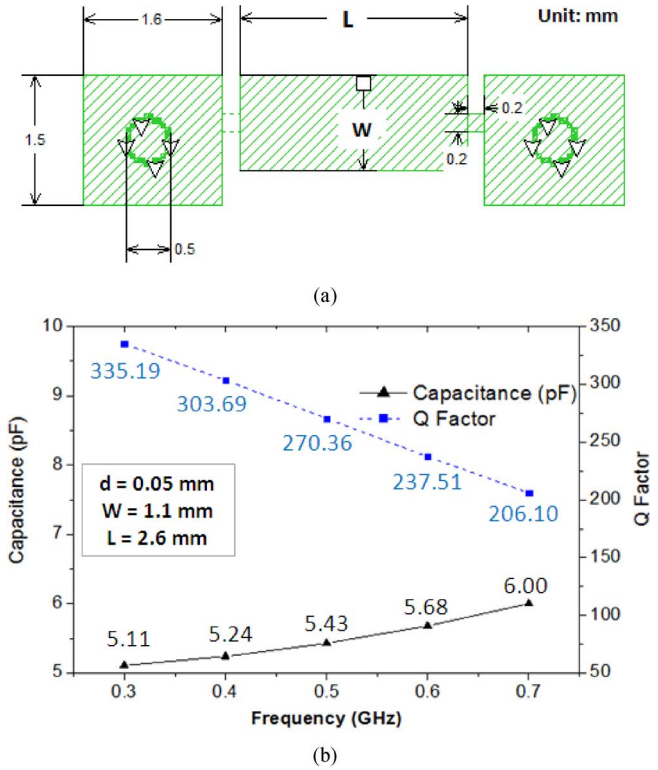

Fig. 4. (a) Planar dimensions for multilayer capacitor. (b) Capacitances and Q factors extracted from simulation at different frequencies with $\epsilon_r = 3$, $h = 0.6$ mm, $\tan\delta = 0.0025$, and $\sigma = 5.8 \times 10^7$ S/m.

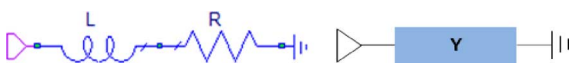

Fig. 5. One-port model for grounding inductor.

shunt to ground, the value extraction process is slightly changed to a one-port model, as shown in Fig. 5. Y_{11} is then the parameter to be used for value extraction due to the short-circuit condition, as shown in (2) and (3). For this work, a spiral line with dimensions as shown in Fig. 6(a) has been chosen. The grounding via has a length of 0.6 mm, which is also the total thickness of the substrate. The central via and via patch sizes are firstly fixed to ensure easy fabrication, then by increasing the number of turns, different inductances can be achieved. Fig. 6(b) shows the inductances, extracted from simulation, for different number of turns and dimensions at the cutoff frequency 0.5 GHz. It can be seen that an inductor with three turns of 0.15-mm-wide line should be used for this work. Fig. 6(c) shows the inductances and Q factors, extracted from simulation, of the selected spiral line at different frequencies

$$Z = R + j\omega L = \frac{1}{Y} = \frac{1}{Y_{11}} \tag{2}$$

$$L = \frac{\mathrm{Im}(Z)}{\omega} = \frac{\mathrm{Im}(1/Y_{11})}{\omega}. \tag{3}$$

By using these elements, an HP filter with cutoff frequency of 0.5 GHz can be built with a 3-D structure, as shown in Fig. 7(a),

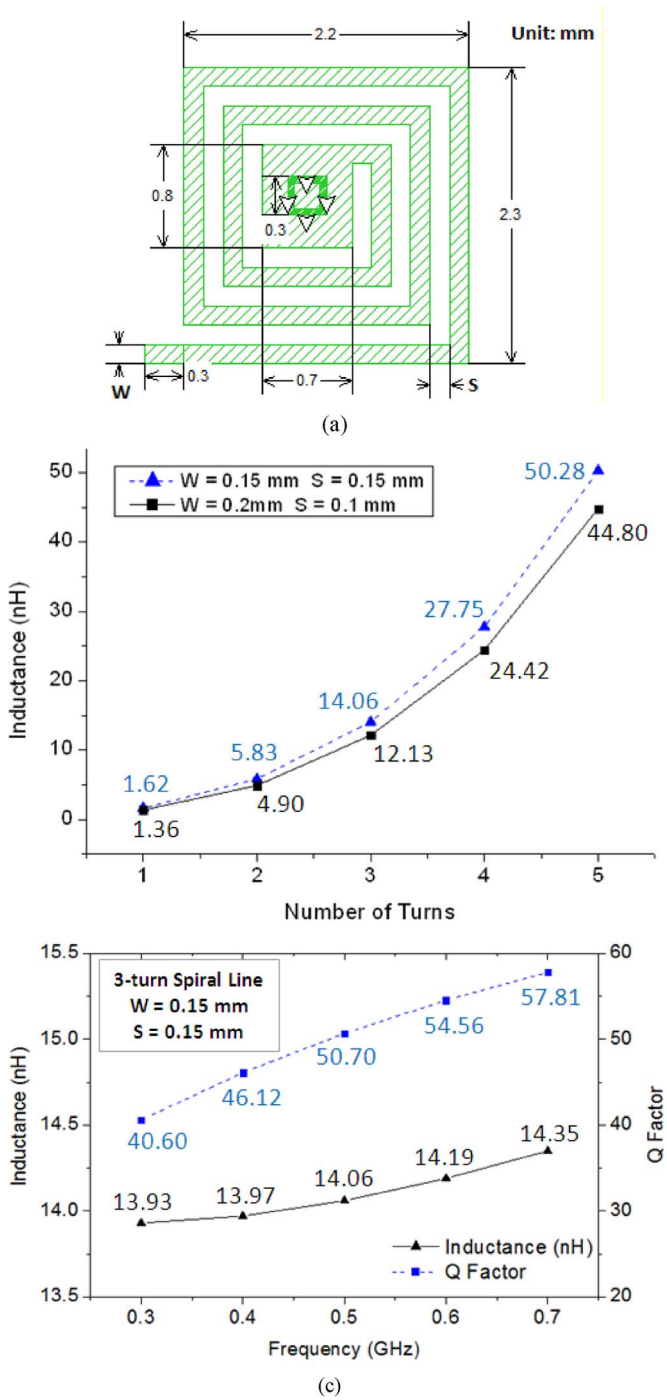

Fig. 6. (a) Planar dimensions for a spiral inductor. (b) Inductances extracted from simulation for the spiral inductor with different number of turns at the cutoff frequency 0.5 GHz. (c) Inductances and Q factors extracted from simulation at different frequencies with $\varepsilon r = 3$, $h = 0.6$ mm, $\tan\delta = 0.0025$, and $\sigma = 5.8 \times 10^7$ S/m.

which has a topology for a small footprint while minimizing parasitic coupling between adjacent elements. Fig. 7(b) shows the full-wave EM simulated result of the proposed structure, compared with the theoretical response of the ideal circuit prototype. The EM simulation was done using commercially available software [21]. It can be seen that the simulated and theoretical transmission or $S21$ responses are almost identical over a very wide frequency range from dc up to 6 GHz, which is

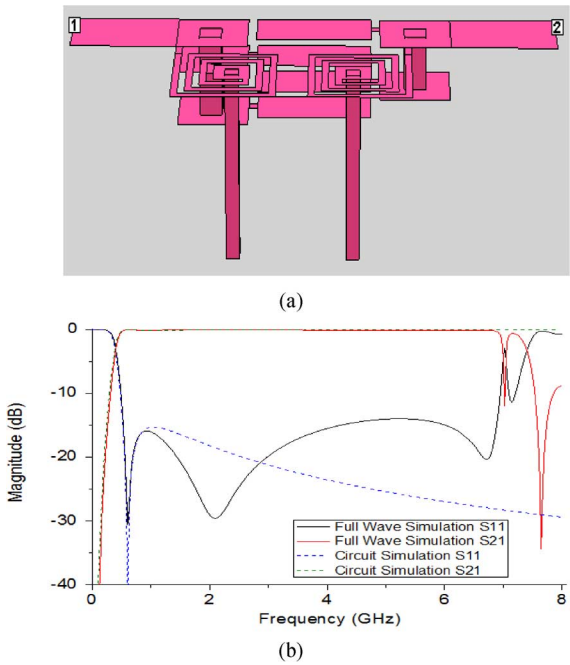

Fig. 7. (a) 3-D structure of the HP section (not on scale). (b) Its full-wave simulation result compared to the circuit model response.

12 times the cutoff of 0.5 GHz. Similarly, the simulated $S11$ or return-loss response is nearly below -15 dB over the wide passband, as predicted by the theory; despite more ripples appearing in the simulated response. It can be shown that these additional ripples mainly result from the parasitic parameters of the microstrip quasi-lumped elements and the spurious resonances around 7 GHz in the simulation are attributed to the self-resonance of the capacitor and inductor. Nevertheless, the designed quasi-lumped elements and their modeling equivalent circuit work well for this wideband filter design.

B. LP Section Design

For the LP section design, a simple LP π network can also be used to produce the LP response with minimum number of elements. However, the passband edge of a conventional Chebyshev LP filter would be very poor compared to the HP section because its transmission zero is at the infinite frequency, which is far away from the desired cutoff frequency of 2 GHz. Thus, for the consideration of getting roughly symmetrical passband edges at both sides, an elliptic-function LP prototype, as shown in Fig. 3(a), is chosen for the LP section to produce a finite-frequency transmission zero near the upper side edge of the passband, as shown in Fig. 3(b).

For the implementation of this LP section, the desired inductor $L2$ with a very small value of 2.48 nH, can be easily implemented with a meander high-impedance line, as shown in Fig. 2(a), with a width of 0.2 mm and a separation of 0.4 mm between the two parallel meandered arms having a length of 2.1 mm. These dimensions are determined from the parameter extraction based on EM simulation. The extracted Q factor for this small inductor is about 78 at the cutoff frequency of 2 GHz.

To realize $C2$, a three-layer small size capacitor can be used because of its small value. The values extracted from simulation are shown in Fig. 8, where W and L are the dimensions as denoted in Fig. 4(a). $C3$ can be implemented with a conventional two-layer broadside coupled structure, with the second layer connected to ground.

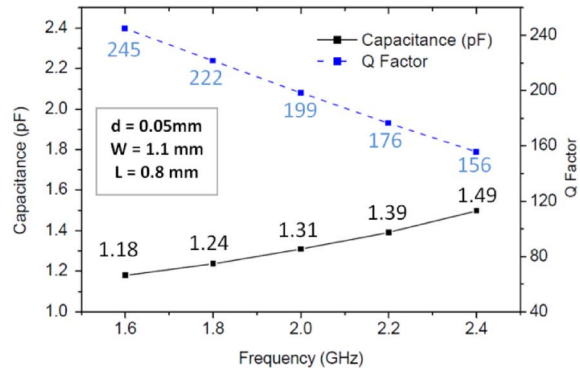

Fig. 8. Capacitances and Q factors extracted from simulation for different frequencies with $\varepsilon_r = 3, h = 0.6$ mm, $\tan\delta = 0.0025$, and $\sigma = 5.8 \times 10^7$ S/m.

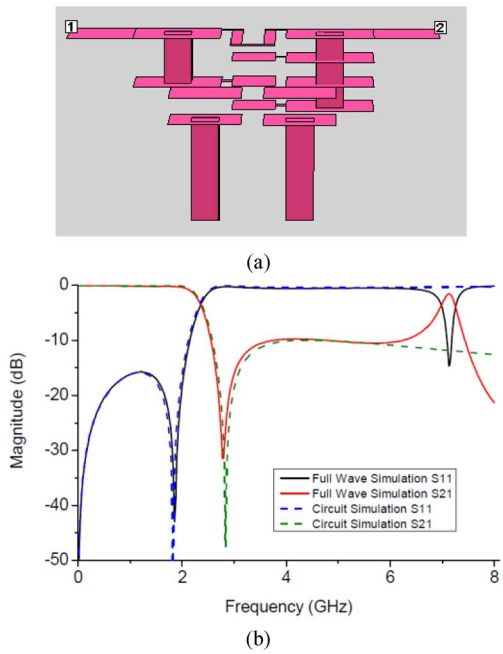

Fig. 9. (a) Proposed 3-D structure for the LP section (not on scale). (b) Its full-wave simulated result compared with the circuit model response.

Based on these elements, the 3-D structure for the LP section can be obtained as shown in Fig. 9(a). Care should be taken to achieve a small size while minimizing unwanted cross couplings by adjusting the separation of the quasi-lumped elements implemented. Fig. 9(b) shows the full-wave simulation result compared to the circuit response. It can be seen that the proposed structure matches well with the circuit response from very low frequency up to 6 GHz.

IV. Multilayer LCP Fabrication

A. LCP Lamination Process

Commercially available LCP substrates can be generally divided into two types: core films and bonding films. Both of them

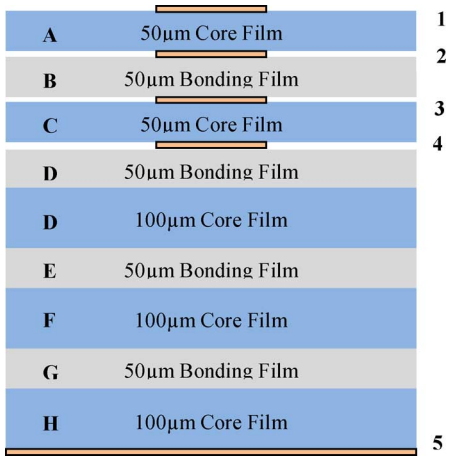

Fig. 10. Five-metal-layer LCP stack up.

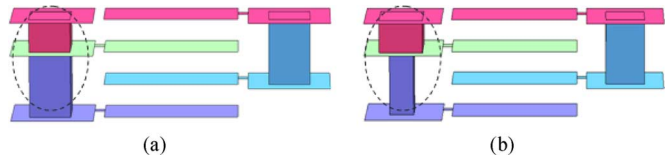

Fig. 11. (a) Conventional and (b) modified inter-connection via structure.

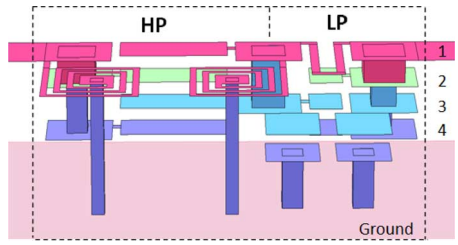

Fig. 12. 3-D structure of the proposed design (not on scale).

have the same dielectric constant and loss tangent. However, the bonding film has a melting temperature of 280 °C, which is lower than that of 315 °C for the core film. Thus, for a multilayer circuit construction, the core films are used as circuit boards, which can be double-side etched by normal inexpensive PCB etching process, while every bonding film is used as an adhesive layer between two core films. Fig. 10 shows a five-metal-layer construction for this work. Metal layers 1–4 are all double-sided etched on 50-μm core films to implement the multilayer circuit structure , while metal layer 5 works as the ground plane.

In addition to the normal lamination guidelines in [22], the registration error (or shift) among stacked LCP layers could be reduced by using the following methods.

1) In general, the less number of layers, the better the registration. For the structure in Fig. 10, since it is only important to get a good registration among the first three layers A–C, which consist of all the circuit metallization, they can be laminated together first. A second lamination can then be done to achieve the required thickness with the ground on the bottom.
2) During the heating process, the high pressure of 300 psi should only be applied after the material has reached 260 °C for half an hour. Otherwise, the circuit metallization can be easily pushed away during the heating process if high pressure is applied at the beginning.
3) The LCP bonding films are thermoplastic adhesive materials so pressure drop during the cooling process can cause large registration error. Thus, the lamination pressure should be kept until the cooling is finished.

B. Inter-Layer via Fabrication Technique

When the multilayer structure is involved, the fabrication complexity is increased. Especially in the case of the multilayer broadside-coupled capacitor, as shown in Fig. 11(a), the fabrication of inter-layer connection via becomes very important for achieving good agreement between fabrication and simulation.

Due to the thermoplastic nature, the LCP bonding films will be melted during the lamination, thus it is not a good solution to drill and fill the vias on separate layers before lamination. For this work, two kinds of inter-layer via fabrication process for LCP have been investigated.

1) After laminating the first three layers A–C, via-holes in Fig. 11(a) can be drilled. By using through-hole plating technique, the inner wall of the vias can be wholly plated by high-conductivity paste. Before doing the second lamination, to prevent the processed vias on the first three layers refilled by the bonding material from layer D under high lamination pressure, via-holes with slightly bigger diameter should be drilled on the layer D at the same positions.
2) Via-holes can also be processed after the whole lamination is done. In this way, via-holes in Fig. 11(a) will be drilled as blind holes. High-conductivity paste can then be applied to the via-holes for metallization.

For the first method, the through holes are easy to be drilled and plated, but the final interconnection depends on the robustness of the plated metallization. The second method provides good connection, but as a tradeoff, it requires more accurate fabrication control to get the blind holes. In this work, the second method is used and all the machining work are done using picosecond laser for precise fabrication. To further improve the connection, all the multilayer interconnection vias are modified to the structure in Fig. 11(b), where the step via has been used to replace the straight via in Fig. 11(a) so that the middle layer can get sufficient contact after applying the paste.

V. Result and Further Improvement

A. Structure and Dimensions

Based on the value extraction process for the microstrip inductors and multilayer broadside-coupled capacitors with the newly developed stepped via connections, the dimensions for the proposed design and 3-D structure have been finalized, as illustrated in Fig. 12. The size of the filter is only 9 mm $\times$ 4 mm $\times$ 0.6 mm, which is $0.058\ \lambda_g \times 0.026\ \lambda_g \times 0.004\ \lambda_g$, and λ_g is the guided wavelength on a 0.6-mm thickness substrate with dielectric constant 3, at the center frequency of 1.25 GHz.

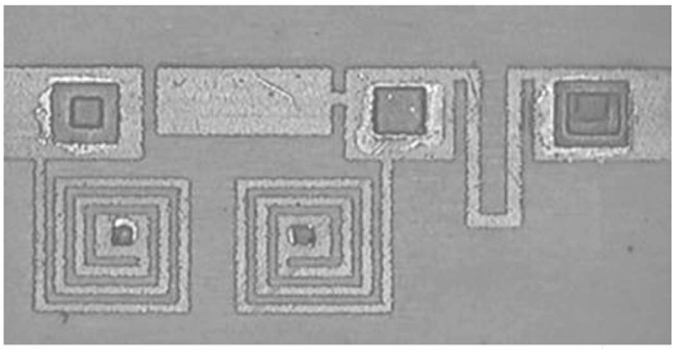

(a)

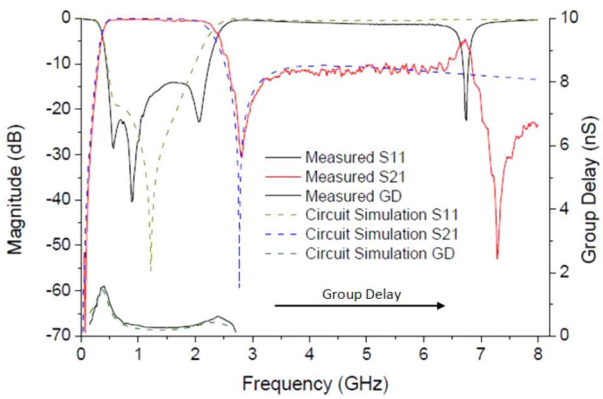

(b)

Fig. 13. (a) Photograph of the fabricated wideband bandpass filter using multilayer LCP technology. (b) Measured result compared with circuit simulation.

The filter is fabricated and measured on a Hewlett-Packard 8510B network analyzer. Fig. 13(a) is a photograph of the fabricated filter. The stepped vias show very good alignment among different layers, which means the registration error has been well controlled during the fabrication. Fig. 13(b) shows the measured result compared to the circuit simulation. Apart from some mismatching problem in the passband, there is only a small frequency shift at the higher cutoff, which is due to fabrication tolerance. Nevertheless, the measurement is in good agreement with the circuit simulation up to 6.5 GHz, which is about five times the center frequency. The insertion loss is smaller than 0.7 dB between 0.5–2 GHz and the group-delay variation is within 0.3 ns between 0.6–1.9 GHz, which is 87% of the passband.

B. Further Improvement

Although the design in Fig. 12 realizes the required passband performance with transmission zeros at both sides of the passband, the upper stopband attenuation is only slightly better than 10 dB. To improve the rejection in the stopband, one could increase the order of the LP filter. This method enhances both the passband and stopband responses; hence, both the passband edge selectivity and stopband rejection can be improved. However, this will introduce more passive elements into the design, which would not only increase the size, but also the insertion loss.

As a compromise, the circuit prototype in Fig. 14(a) is adopted as an improved design. Compared to the original

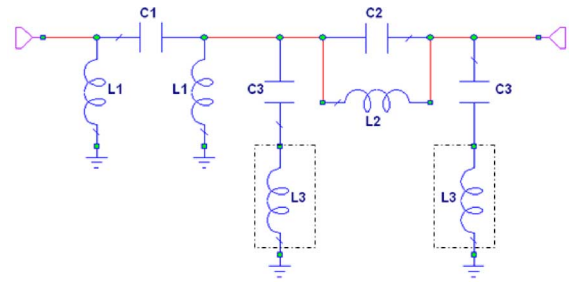

(a)

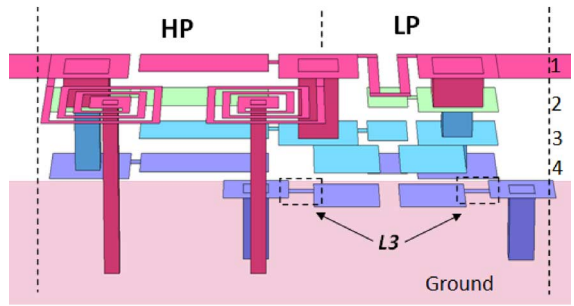

(b)

Fig. 14. (a) Modified circuit prototype and (b) its 3-D structure (not on scale) ($C1 = 5.5$ pF, $L1 = 14.3$ nH, $C2 = 1.33$ pF, $L2 = 2.48$ nH, $C3 = 1.19$ pF, $L3 = 0.85$ nH).

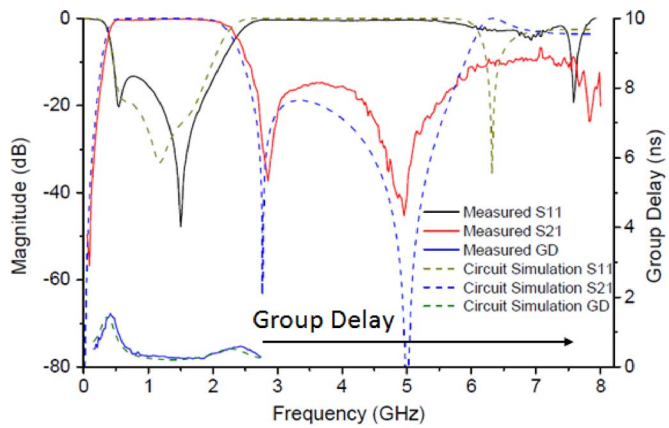

Fig. 15. Measured and circuit simulated response of the improved design with improved stopband performance.

circuit in Fig. 3(a), this design adds only one more inductor to each of the shunt branches and this works together with the shunt capacitor as a series resonator to the ground, which can produce another transmission zero in the stopband while keeping the passband response almost unchanged.

Another advantage of this improved prototype is it is easy to implement the extra inductors on the original microstrip layout. It only changes the fourth layer with a pair of high-impedance lines, as shown in Fig. 14(b). The total size is 10 mm $\times$ 4 mm $\times$ 0.6 mm, which is $0.065\ \lambda_g \times 0.026\ \lambda_g \times 0.004\ \lambda_g$, and λ_g is the guided wavelength on a 0.6-mm thickness substrate with dielectric constant 3, at the center frequency 1.25 GHz. This improved design has also been fabricated and the layout is almost the same as that shown in Fig. 13(a). The filter is measured on a Hewlett-Packard 8510B network analyzer and the result is

shown in Fig. 15. It can be seen that the passband has better than 13-dB return loss and 0.7-dB insertion loss. The upper stopband has been improved with better than 17-dB attenuation up to 6 GHz and 10-dB attenuation is achieved until 7 GHz. The measured group delay also matches the simulation with a variation within 0.3 ns. Compared to the circuit simulation result, there is a little frequency shift in the higher cutoff and the stopband attenuation has been decreased slightly due to fabrication tolerance. From the measured result of the two filters in this work, it can be seen that due to the smaller size of the elements, the LP filter that controls the high side of the passband and the upper stopband is more sensitive to the fabrication tolerances. This explains why both measured results show slight frequency shift at the higher cutoff.

VI. Conclusion

In this paper, two compact high-performance wideband filters have been designed and fabricated using the promising multilayer LCP technology. With the presented design methodology, the values of microstrip lumped elements can be accurately extracted and the whole filter can be then designed efficiently with less EM optimization time.

Besides, a five-metal-layer LCP structure has been presented in this paper, which has not been done before for the design of multilayer LCP filters and the newly developed fabrication technique has also been detailed.

However, further size reduction can still be achieved in future. In this design, via-hole sizes are relatively large as it is needed for the stepped via connection. This also results in very large via patches. In the future, with better plating technique, smaller via-hole sizes can be used, and thus the overall size of the filter can be reduced further.

Acknowledgment

The authors are grateful to Z.-C. Hao, F. Albri, J. Parry, D. Hand, M. I. Mohammed, and S. Wilhelm, all with the School of Engineering and Physical Sciences, Heriot-Watt University, Edinburgh, U.K., for their help and support in this work.

References

[1] Y.-X. Guo, L. C. Ong, M. Y. W. Chia, and B. Luo, "Dual-band bandpass filter in LTCC," in *IEEE MTT-S Int. Microw. Symp. Dig.*, 2005, pp. 2219–2222.

[2] H. Joshi and W. J. Chappell, "Dual-band lumped-element bandpass filter," *IEEE Trans. Microw. Theory Tech.*, vol. 54, no. 12, pp. 4169–4177, Dec. 2006.

[3] M. Hoft and T. Shimamura, "Design of symmetric trisection filters for compact low-temperature co-fired ceramic realization," *IEEE Trans. Microw. Theory Tech.*, vol. 58, no. 1, pp. 165–175, Jan. 2010.

[4] C.-W. Tang and D.-L. Yang, "Realization of multilayered wide-passband bandpass filter with low-temperature co-fired ceramic technology," *IEEE Trans. Microw. Theory Tech.*, vol. 56, no. 7, pp. 1668–1674, Jul. 2008.

[5] T. H. Duong and I. S. Kim, "New elliptic funtion type UWB BPF based on capacitively coupled $\lambda/4$ open T resonator," *IEEE Trans. Microw. Theory Tech.*, vol. 57, no. 12, pp. 3089–3098, Dec. 2009.

[6] S. Hwang, S. Min, M. Swaminathan, V. Venkatakrishnan, H. Chan, F. Liu, V. Sundaram, S. Kennedy, D. Baars, B. Lacroix, Y. Li, and J. Papapolymerou, "Characterization of next generation thin low-k and low-loss organic dielectrics from 1 to 110 GHz," *IEEE Trans. Adv. Packag.*, vol. 33, no. 1, pp. 180–188, Feb. 2010.

[7] S. Hwang, S. Min, M. Swaminathan, V. Sundaram, and R. Tummala, "Thin-film high-rejection filter integration in low-loss organic substrate," *IEEE Trans. Compon. Packag. Manuf. Technol.*, vol. 1, no. 8, pp. 1160–1170, Aug. 2011.

[8] K. Brownlee, S. Bhattacharya, K. Shinotani, C. P. Wong, and R. Tummala, "Liquid crystal polymer for high performance SOP applications," in *8th IEEE Int. Adv. Packag. Mater. Symp.*, Mar. 3–6, 2002, pp. 249–253.

[9] D. C. Thompson, O. Tantot, H. Jallageas, G. E. Ponchak, M. Tentzeris, and J. Papapolymerou, "Characterization of liquid crystal polymer (LCP) material and transmission lines on LCP substrate from 30–100 GHz," *IEEE Trans. Microw. Theory Tech.*, vol. 52, no. 4, pp. 1343–1352, Apr. 2004.

[10] Z.-C. Hao and J.-S. Hong, "Ultra-wideband bandpass filter using multilayer liquid-crystal-polymer technology," *IEEE Trans. Microw. Theory Tech.*, vol. 56, no. 9, pp. 2095–2100, Sep. 2008.

[11] Z.-C. Hao and J.-S. Hong, "UWB bandpass filter using cascaded miniature high-pass and low-pass filters with multilayer liquid crystal polymer technology," *IEEE Trans. Microw. Theory Tech.*, vol. 58, no. 4, pp. 941–948, Apr. 2010.

[12] Z.-C. Hao and J.-S. Hong, "Ultra wideband bandpass filter using embedded stepped impedance resonators on multilayer liquid crystal polymer substrate," *IEEE Microw. Wireless Compon. Lett.*, vol. 18, no. 9, pp. 581–583, Sep. 2008.

[13] Z.-C. Hao and J.-S. Hong, "Compact wide stopband ultra wideband bandpass filter using multilayer liquid crystal polymer technology," *IEEE Microw. Wireless Compon. Lett.*, vol. 19, no. 5, pp. 290–292, May 2009.

[14] S. Mukherjee, B. Mutnury, S. Dalmia, and M. Swaminathan, "Layout-level synthesis of RF inductors and filters in LCP substrates for Wi-Fi applications," *IEEE Trans. Microw. Theory Tech.*, vol. 58, no. 4, pp. 2196–2210, Apr. 2005.

[15] G.-S. Huang, Y.-S. Lin, C.-H. Wang, and C. H. Chen, "A novel transition-included multilayer filter," *IEEE Trans. Microw. Theory Tech.*, vol. 57, no. 4, pp. 807–814, Apr. 2009.

[16] S. Qian, Z.-C. Hao, J.-S. Hong, J. P. Parry, and D. P. Hand, "Design and fabrication of a miniature highpass filter using multilayer LCP technology," in *Proc. 41th Eur. Microw. Conf.*, Oct. 2011, pp. 187–190.

[17] J.-S. Hong, *Microstrip Filters for RF/Microwave Applications*, 2nd ed. Hoboken, NJ: Wiley, 2011.

[18] I. Bahl, *Lumped Element for RF and Microwave Circuits*. Boston, MA: Artech House, 2003.

[19] G. Brzezina, L. Roy, and L. MacEachern, "A miniature LTCC bandpass filter using novel resonators for GPS applications," in *Proc. 37th Eur. Microw. Conf.*, Oct. 2007, pp. 536–539.

[20] S. S. Mohan, M. del Mar Hershenson, S. P. Boyd, and T. H. Lee, "Simple accurate expressions for planar spiral inductances," *IEEE J. Solid-State Circuits*, vol. 34, no. 10, pp. 1419–1424, Oct. 1999.

[21] *"EM User's Manual,"* ver. 12, Sonnet Softw. Inc., 2010, Syracuse, NY.

[22] "Fabrication guidelines ULTRALAM-3000-LCP-materials," Rogers Corporation, Rogers, CT, 2012.

Shilong Qian (S'10) was born in Wuhan, China, in 1987. He received the B.Eng. degree in communications engineering from the Huazhong University of Science and Technology, Wuhan, China, in 2009, and is currently working towards the Ph.D. degree at the School of Engineering and Physical Sciences, Heriot-Watt University, Edinburgh, U.K.

He is currently with the Department of Electrical, Electronic and Computer Engineering, Heriot-Watt University. His research interests include miniature RF/microwave filters, reconfigurable filters and multilayer circuit packaging, and integration for wireless communication systems.

Jiasheng Hong (M'94–SM'05–F'12) received the D.Phil. degree in engineering science from the University of Oxford, Oxford, U.K., in 1994. His doctoral dissertation concerned EM theory and applications.

In 1994, he joined the University of Birmingham, Birmingham, Edgbaston, U.K., where he was involved with microwave applications of high-temperature superconductors, EM modeling, and circuit optimization. In 2001, he joined the Department of Electrical, Electronic and Computer Engineering, Heriot-Watt University, Edinburgh, U.K., where he is currently a Professor leading a team for research into advanced RF/microwave device technologies. He has authored or coauthored over 200 journal and conference papers and *Microstrip Filters for RF/Microwave Applications* Wiley, 2001, 1st ed, 2011, 2nd ed) and *RF and Microwave Coupled-Line Circuits, Second Edition* (Artech House, 2007). His current interests involve RF/microwave devices such as antennas and filters for wireless communications and radar systems, as well as novel material and device technologies including multilayer circuit technologies using package materials such as LCP, RF microelectromechanical systems (MEMS), and ferroelectric and high-temperature superconducting devices.